Supporting Information for

Solar-driven CO_2 reduction catalysed by Hybrid Supramolecular Photocathodes and enhanced by Ionic Liquids

Roger Miró,[a] Hilmar Guzmán,[b] Cyril Godard,*[c] Aitor Gual,*[a] Federica Zammillo,[b] Thomas J.S. Schubert,[d] Boyan Iliev,[d] Angelica Chiodoni,[d] Simelys Hernández,*[b] Miriam Díaz de los Bernardos*[a]

a) Unitat de Tecnologies Químiques, Fundació Eurecat - Centre Tecnològic de Catalunya, Tarragona, 43007, Spain.

(b) CREST Group, Department of Applied Science and Technology (DISAT), Politecnico di Torino, Turin, Italy.

(c) Departament de Química Física i Inorgànica, Universitat Rovira i Virgili, Tarragona, 43007, Spain

(d) Center for Sustainable Future Technologies (IIT@Polito), Italian Institute of Technology, Turin, Italy.

Table of contents

SI. General considerations

Reagents: Commercially available reagents and solvents were purchased at the highest commercial quality from Sigma-Aldrich, Fisher scientific, Alfa Aesar and were used as received, without further purification, unless otherwise stated.

Analytical methods: ^{1}H, and $^{13}C\{^{1}H\}$ NMR spectra were recorded using a Varian Mercury VX 400 (400 and 100.6 MHz respectively). Chemical shift values (δ) are reported in ppm relative to TMS (^{1}H and $^{13}C\{^{1}H\}$), and coupling constants are reported in Hertz. The following abbreviations are used to indicate the multiplicity: s, singlet; d, doublet; t, triplet; q, quartet; m, multiplet; bs, broad signal.

High-resolution mass spectra (HRMS) were recorded on an Agilent Time-of-Flight 6210 using ESI-TOF (electrospray ionization-time of flight). Samples were introduced to the mass spectrometer ion source by direct injection using a syringe pump and were externally calibrated using sodium formate. The instrument was operating in the positive ion mode.

Fourier transform infrared spectroscopy (FT-IR) spectra were obtained by using a Bruker Vertex-70 instrument with Attenuated Total Reflectance (ATR) sample holder by acquiring 16 cumulative scans with resolution of 4 cm^{-1} from 4000 to 400 cm^{-1}.

Ultraviolet-visible (UV-Vis) absorption spectra (350 nm to 800 nm) were recorded of the synthetized molecules in standard solutions 30 mg/L in dichloromethane. Analyses were carried out using quartz cuvette with 1 cm of optical path using a UV-1800 Shimadzu apparatus.

Reactions were monitored by TLC carried out on 0.25 mm E. Merck silica gel 60 F254 glass or aluminum plates. Developed TLC plates were visualized under a short-wave UV lamp (254 nm) and by heating plates that were dipped in potassium permanganate. Flash column chromatography was carried out using forced flow of the indicated solvent on Merck silica gel 60 (230-400 mesh).

Synthesis: The following organic ligands were synthetized as described in the literature. 4,4'-Divinyl-2,2'-bipyridine[1], 1,2-bis(4'-methyl-[2,2'-bipyridin]-4-yl)ethane[2].

SII. $CuGaO_2$ XRD

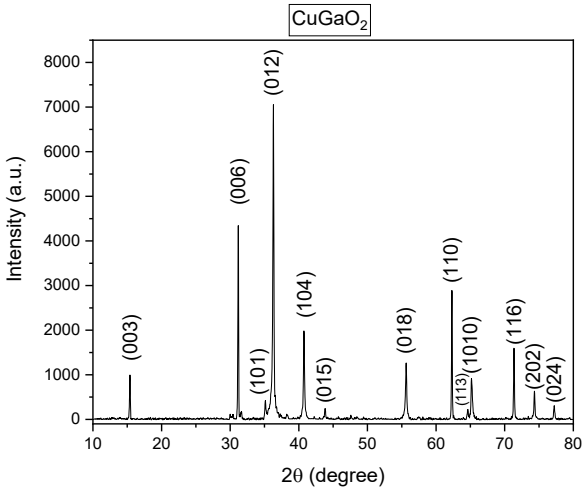

***Figure S1**: XRD analysis of $CuGaO_2$.*[3]

SIII. EDX analysis of $CuGaO_2$

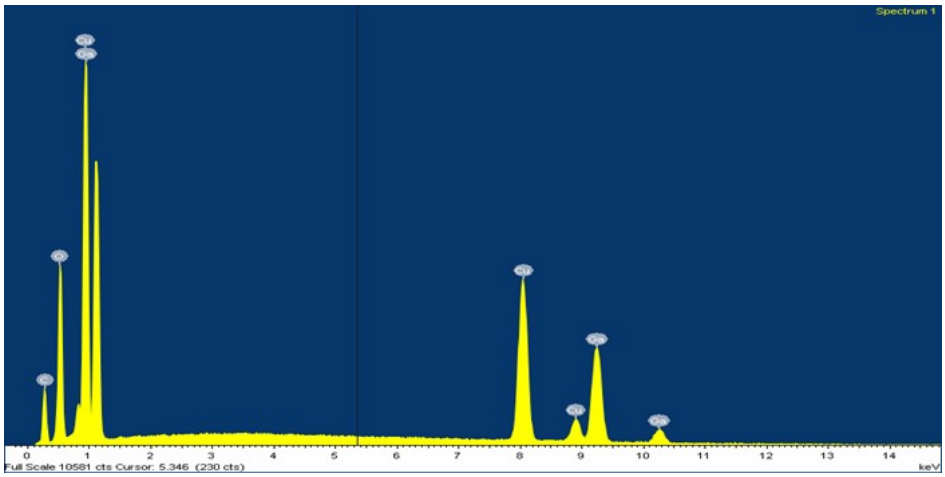

***Figure S2**: EDX analysis of $CuGaO_2$.*

SIV. FESEM-EDX analysis of $CuGaO_2$-VTES

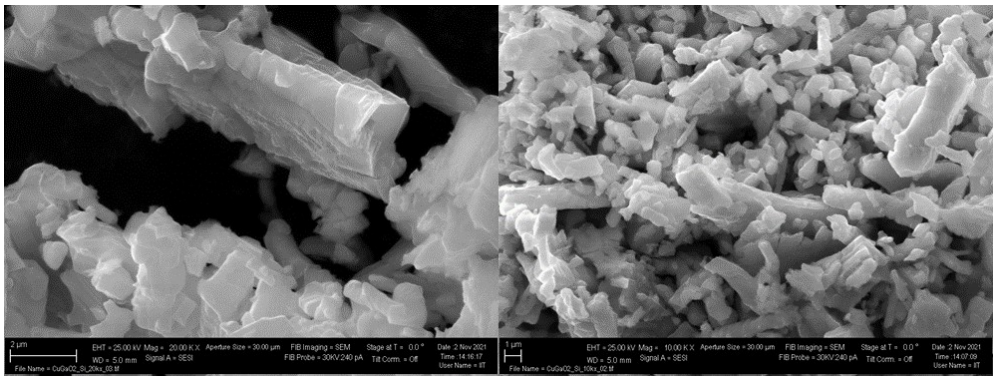

***Figure S3**: FESEM images of $CuGaO_2$-VTES.*

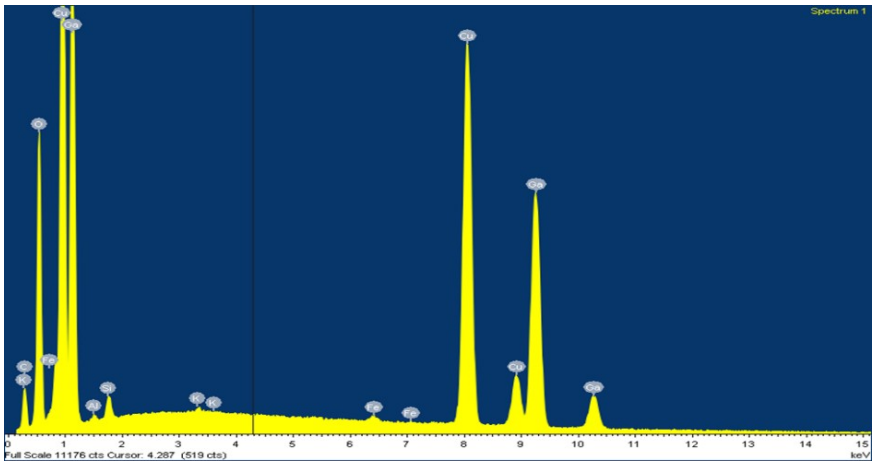

***Figure S4**: EDX analysis of $CuGaO_2$-VTES.*

SV. Ru visible light absorber synthesis.

The synthesis of the Ru visible light absorber (**Ru_{VLA}**) was performed following the synthetic route of Figure S5. The **Ru_{VLA}** complex was synthetized with an overall isolated yield of 74%.

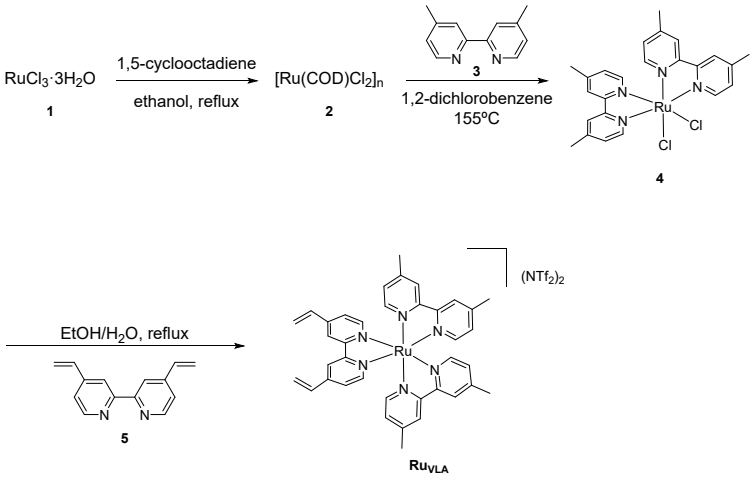

***Figure S5**: Ruthenium visible light absorber synthetic route*

The synthesis starts with the commercial $RuCl_3 \cdot 3H_2O$ precursor. The first step is the preparation of the polymeric $[Ru(COD)Cl_2]_n$ **2** where the $RuCl_3$ is reduced to Ru(II). The next step is the substitution of the COD ligand for two bipyridines ligand **3** obtaining the corresponding $Ru(Me_2bpy)_2Cl_2$ **4**. Finally, the substitution of the two Cl ligands for the bipyridine with the vinyl group take place obtaining the final Ru visible light absorber.

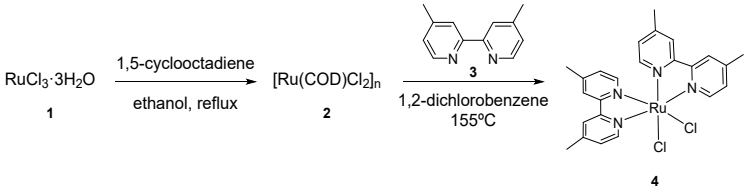

***Figure S6**: Synthesis of $[Ru(Me_2bpy)_2Cl_2]$ **4**, two-step procedure.*

cis-$[Ru(Me_2bpy)_2Cl_2]$ 4: The synthesis was performed according to an adapted reported procedure.[4] $RuCl_3 \cdot 3H_2O$ (0.55 g, 2.7 mmol) was added to a mixture of 1,5-cyclooctadiene (3.25 mL, 27 mmol) and ethanol (12 mL), and refluxed under argon atmosphere for 64 h. After cooling

to room temperature, resulting precipitates were collected by filtration affording dichlorido(1,5-cyclooctadiene)ruthenium(II) polymer ($[Ru(COD)Cl_2]_n$) **2** as brown solid (0.52 g, 88%). A suspension of $[Ru(COD)Cl_2]_n$ **2** (0.251 g, 0.89 mmol) and Me_2bpy **3** (0.332 g, 1.8 mmol) in o-dichlorobenzene (3.8 mL) was stirred at 155ºC under argon-gas atmosphere for 3.5 h. After cooling to room temperature, resulting precipitates were collected by filtration and dried in vacuo, afforded $[Ru(Me_2bpy)_2Cl_2]$ **4** as black powders (0.43 g, 84%). This compound was used in the following step without any purification and identification.

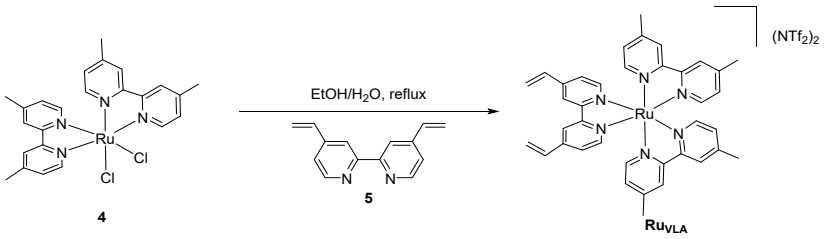

***Figure S7**: Second synthesis step of the Ru_{VLA}.*

Ru_{VLA}: The synthesis was performed according to an adapted reported procedure.[5] A solution of the ligand **5** (104.13 mg, 0.5 mmol) and (324.3 mg, 0.6 mmol) of **4** in a 50 mL mixture of $EtOH/H_2O$ (9:1 v:v) was heated at reflux in the dark under an argon atmosphere for 3 h. The solvents were removed, and the product was purified on silica gel column. Elution with an acetone/water mixture (8:2 v:v) removed the unreacted $Ru(Me_2bpy)_2Cl_2$. More rinsing with an acetone/water/KNO_3 saturated aqueous solution (10 drops of KNO_3 added to a mixture of 80 mL of acetone and 20 mL of water) afforded the desired ester complex with NO_3^- as counteranion. The pure fractions of the product were collected and evaporated under reduced pressure. The product was redissolved with dichloromethane and 0.2 g of $AgNTf_2$ was added and stirred during 10 min. $MgSO_4$ was added and the organic phase was filtered and dried to give the **Ru_{VLA}** as a red powder (0.36 g, 49 %). **^{1}H NMR** (400 MHz, CD_2Cl_2) d: 2.57 (d, J_{H-H} = 2.5 Hz, 12 H), 5.72 (d, J_{H-H} = 10.8 Hz, 2 H), 6.22 (d, J_{H-H} = 17.5 Hz, 2 H), 6.85 (dd, J_{H-H} = 10.9, 17.5 Hz, 2 H), 7.22 (t, J_{H-H} = 7.8, 4 H), 7.42 (dd, J_{H-H} = 1.7, 6.0 Hz, 2 H), 7.51 (t, J_{H-H} = 5.5 Hz, 4 H), 7.62 (d, J_{H-H} = 6.0 Hz, 2 H), 8.22 (s, 4 H), 8.34 (s, 2 H). **^{13}C{^{1}H} NMR** (100.6 MHz, CD_2Cl_2) d: 21.5, 115.5, 118.6, 121.4, 121.8, 122.9, 124.6, 125.0, 125.3, 128.8, 129.1, 129.2, 133.1, 146.9, 150.6, 150.7, 150.8, 150.9, 151.4, 156.6, 156.7, 156.8, 157.5. **ESI-HRMS:** Calculated for $C_{38}H_{36}N_6Ru^{2+}$. Exact: M^{2+}: 339.1017; Experimental: M^{2+}: 339.1026.

SVI. Re CO_2 reduction co-catalyst synthesis

The synthesis of this Re complex (**Re_{CAT}**) is performed via one step synthesis using the commercial $Re(CO)_5Br$ precursor and performing the substitution of two CO ligands with one bipyridine ligand **5**.

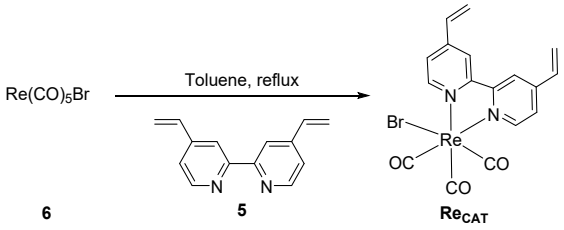

***Figure S8**: Synthesis scheme of the Re_{CAT} complex.*

Re_{CAT}: The synthesis was performed according to an adapted reported procedure.[6] The $Re(CO)_5Br$ **6** (0.1 g, 0.246 mmol) and the ligand **5** (51.21 mg, 0.246 mmol) were dissolved in toluene (60 mL) and stirred at reflux for 3 h. Then, the solvent was evaporated under vacuum and the product precipitated upon the addition of Et_2O. The precipitated was filtered and washed with Et_2O giving the Re complex as an orange solid. 114.7 mg, 84% isolated yield. **^{1}H NMR** (400 MHz, dmso-d_6) d: 5.86 (d, J_{H-H} = 11.0 Hz, 2 H), 6.55 (d, J_{H-H} = 17.6 Hz, 2 H), 6.95 (dd, J_{H-H} = 10.9, 17.6 Hz, 2 H), 7.79 (dd, J_{H-H} = 1.6, 5.8 Hz, 2 H), 8.90 (s, 2 H), 8.94 (d, J_{H-H} = 5.8, 2 H). **^{13}C{^{1}H} NMR** (100.6 MHz, dmso-d_6) d: 121.0, 124.0, 124.5, 133.2, 148.1, 153.2, 155.7, 189.6, 197.4. **ESI-HRMS:** Calculated for $C_{17}H_{16}BrN_3O_3Re^+$. Exact: $(M+NH_4)^+$: 575.9927; Experimental: $(M+NH_4)^+$: 575.9901.

SVII. Supramolecular RuRe1 complex synthesis

The first supramolecular Ru-Re (**RuRe1**) complex was synthetized with the ligand **8** as a linker between the Ru and the Re complex. In this case there is a bridge of two carbons between the Ru and Re. This complex was synthetized with four steps synthesis procedure with an overall isolated yield of 64%.

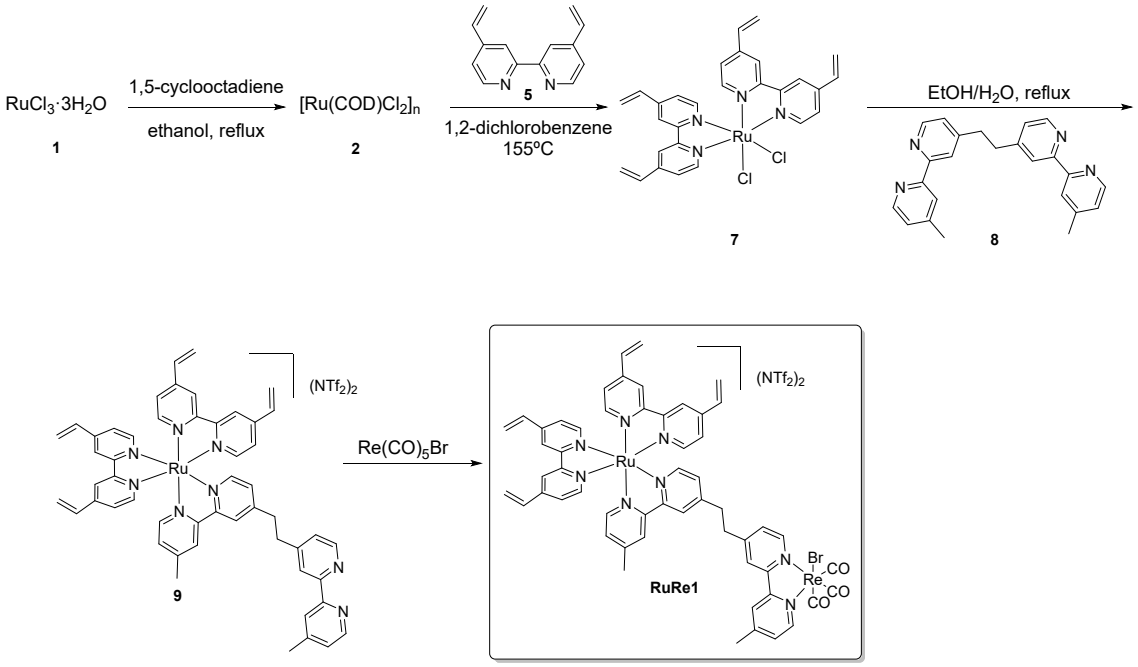

***Figure S9**: Synthetic strategy to synthetize the **RuRe1** complex.*

To synthetize the Supramolecular **RuRe1** a similar strategy than for the synthesis of the Ru visible light absorber is followed but using different organic ligands. And the final step is the coordination of the Re precursor in the molecular complex **9**.

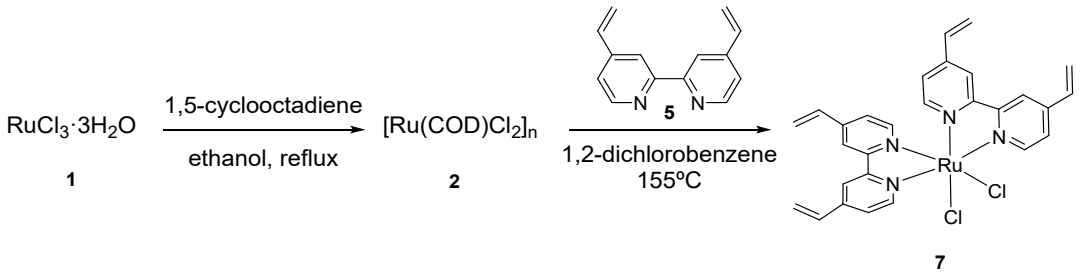

***Figure S10**: Ru complex **7** synthetic route.*

Ru complex 7: The synthesis of the Ru complex is described in the section SV in the Figure S6 but using the ligand **5** (374.9 mg, 1.8 mmol) instead of the ligand **3**. The complex **7** was obtained with an 87% of isolated yield.

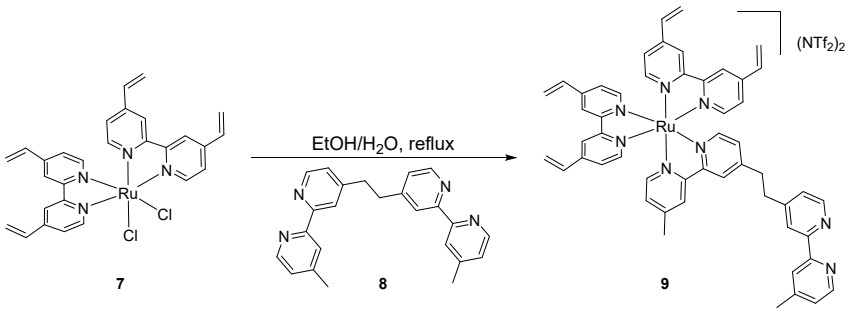

***Figure S11**: Synthesis of Ru complex **9**.*

Ru complex 9: The synthesis was performed according to an adapted reported procedure.[5] A solution of the ligand **8** (259 mg, 0.71 mmol) and (530 mg, 0.85 mmol) of Ru complex **7** in a 71 mL mixture of EtOH/H_2O (9:1 v:v) was heated at 95ºC in the dark under an argon atmosphere for 3 h. The solvents were removed, and the product was purified on silica gel column. Eluting with an acetone/water mixture (8:2 v:v) containing KNO_3 saturated aqueous solution (10 drops of KNO_3 added to a mixture of 80 mL of acetone and 20 mL of water). The pure fractions of the product were collected and evaporated under reduced pressure. The product was redissolved with dichloromethane and 0.27 g of $AgNTf_2$ was added and stirred during 10 min. $MgSO_4$ was added and the organic phase was filtered and dried. The solid was redissolved with acetone and precipitated with diethyl ether to give the pure product **9** as a red powder (0.592 g, 58 %). **^{1}H NMR** (400 MHz, CD_2Cl_2) d: 2.54 (s, 3H), 2.59 (s, 3H), 3.24 (m, 4H), 5.73 (m, 4H), 6.23 (m, 4H), 6.85 (m, 4H), 7.21 (d, J_{H-H} = 5.4 Hz, 1H), 7.33-7.50 (m, 8H), 7.63 (m, 5H), 8.19-8.52 (m, 10H). **^{13}C{^{1}H} NMR** (100.6 MHz, CD_2Cl_2) d: 21.3, 21.4, 35.6, 36.0, 115.4, 118.6, 121.5, 121.6, 121.8, 122.8, 122.9, 123.4, 124.3, 124.7, 124.8, 125.0, 126.0, 126.9, 128.4. 129.1, 133.0, 133.1, 147.0, 147.1, 150.3, 150.7, 150.9, 151.1, 151.4, 151.5, 151.6, 151.9, 152.2, 152.8, 153.2, 153.6, 156.7, 157.1, 157.2, 157.3, 157.4, 157.5. **ESI-HRMS:** Calculated for $C_{52}H_{46}N_8Ru^{2+}$. Exact: M^{2+}: 442.1439; Experimental: M^{2+}: 442.1437.

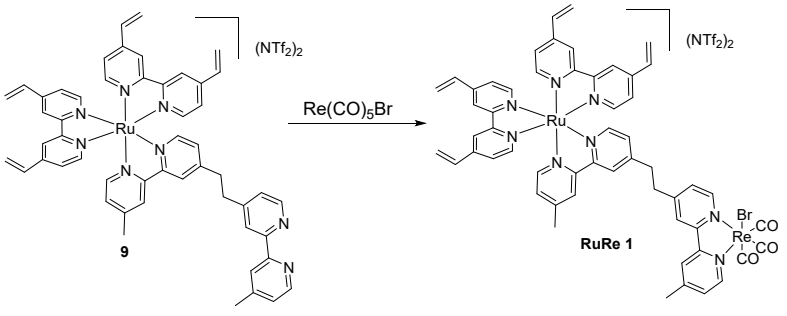

***Figure S12**: Synthesis of the **RuRe1** complex.*

RuRe1: The synthesis was performed according to an adapted reported procedure.[7] 60.7 mg (0.042 mmol) of the Ru complex **9** and 34.12 mg (0.084 mmol) of $Re(CO)_5Br$ were refluxed in a 30 mL mixture acetone/ethanol 1:1 overnight. The solvent was evaporated and the solid was redissolved in the minimum amount of acetone and then precipitated with diethyl ether to obtain the pure RuRe **1** in 48% isolated yield (35.9 mg). **^{1}H NMR** (400 MHz, CD_2Cl_2) d: 2.54 (m,

6H), 3.21 (m, 4H), 5.73 (dd, J_{H-H} = 1.9, 10.9 Hz, 4H), 6.22 (m, 4H), 6.84 (m, 4H), 7.17-7.48 (m, 9H), 7.59 (m, 5H), 8.23-8.50 (m, 8H), 8.76 (m, 2H). **$^{13}C\{^{1}H\}$ NMR** (100.6 MHz, CD_2Cl_2) d: 21.3, 21.5, 35.6, 35.7, 115.4, 118.6, 121.4, 121.6, 121.8, 123.1, 124.4, 124.5, 124.6, 124.7, 124.9, 125.0, 125.2, 126.2, 127.4, 128.3, 128.5, 129.1, 130.0, 133.0, 133.1, 147.0, 147.1, 147.1, 150.2, 151.1, 151.3, 151.4, 151.5, 151.6, 152.4, 152.5, 152.8, 152.9, 154.1. 154.2, 155.6, 155.7, 156.4, 156.4, 156.6, 157.1, 157.3, 157.4, 157.5, 189.6, 197.9, 198.1. **ESI-HRMS:** Calculated for $C_{55}H_{46}BrN_8O_3ReRu^{2+}$. Exact: M^{2+}: 617.0733; Experimental: M^{2+}: 617.0722.

To confirm the correct coordination of the Re complex was performed an IR analysis of the complex before (Ru complex 9) and after the coordination of the Re complex (**RuRe1**).

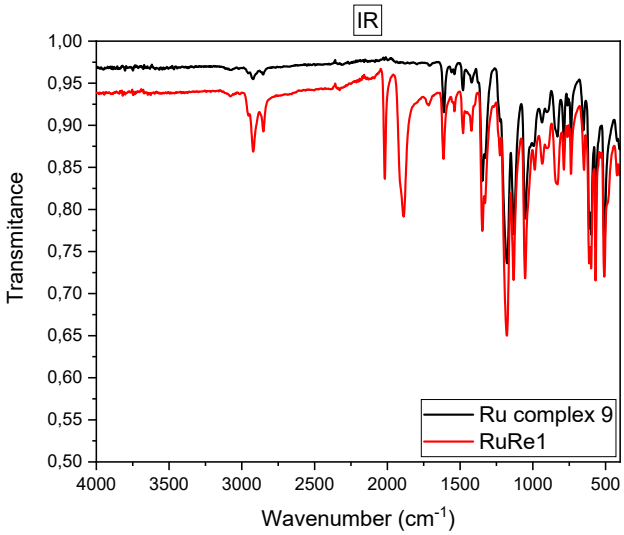

***Figure S13**: IR Spectrum of red) **RuRe1** and black) Ru complex **9**.*

As it can be observed in the Figure S13 in the IR spectrum of the Ru complex 9 there are not any characteristic peak of the CO bond, instead when the Re complex is coordinated is possible to observe two peaks corresponding to the CO bond in 2016 and 1889 cm^{-1}. These peaks confirm the good coordination of the Re complex.

SVIII. Supramolecular RuRe2 complex synthesis

To compare the effect of the ligand between the Ru and Re a new Supramolecular Ru-Re (**RuRe2**) complex was synthetized with the 2,2'-Bipyrimidine **10** as ligand.

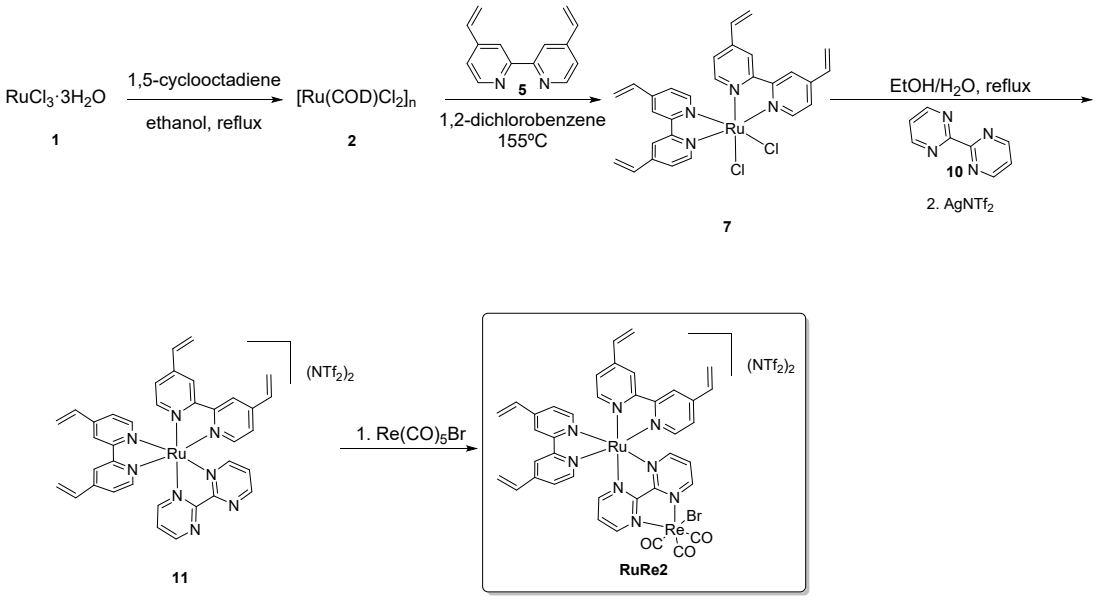

***Figure S14**: Synthesis scheme of the **RuRe2** complex.*

The synthesis of the **RuRe2** complex is very similar than for the **RuRe1** complex. To synthetize the **RuRe2** the 2,2'-Bipyrimidine **10** ligand will be used instead of the ligand **8**. The **RuRe2** complex was obtained with an overall isolated yield of 67%.

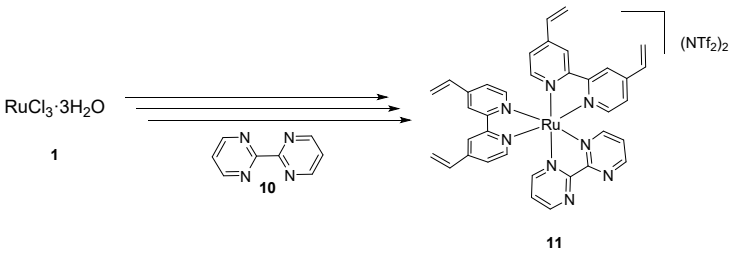

***Figure S15**: Synthesis of Ru complex **11**.*

Ru complex 11: The synthesis procedure of the Ru complex **11** is described in the section SVII. To synthetize the complex **11** the synthesis is performed with the ligand **10** instead of the ligand **8**. The pure Ru complex **11** was obtained in 57% isolated yield (404.5 mg). **^{1}H NMR** (400 MHz, CD_3OD) d: 5.75 (dd, J_{H-H} = 5.0, 10.9 Hz, 4H), 6.39 (dd, J_{H-H} = 4.0, 17.6 Hz, 4H), 6.93 (m, 4H), 7.56 (m, 4H), 7.71 (d, J_{H-H} = 5.9 Hz, 2H), 7.41 (m, 2H), 7.80 (dd, J_{H-H} = 5.0, 5.8 Hz, 2H), 7.93 (d, J_{H-H} = 5.9 Hz, 2H), 8.41 (dd, J_{H-H} = 1.9, 5.8 Hz, 2H), 8.83 (s, 4H), 9.18 (dd, J_{H-H} = 1.9, 4.9 Hz, 2H). **^{13}C{^{1}H} NMR** (100.6 MHz, CD_3OD) d: 119.6, 122.7, 122.8, 122.9, 123.3, 125.6, 125.8, 126.8, 134.3, 134.3, 149.0, 152.5, 153.4, 158.5, 158.7, 159.2, 162.0, 162.7. **ESI-HRMS:** Calculated for $C_{36}H_{30}N_8Ru^{2+}$. Exact: M^{2+}: 338.0813; Experimental: M^{2+}: 338.0816.

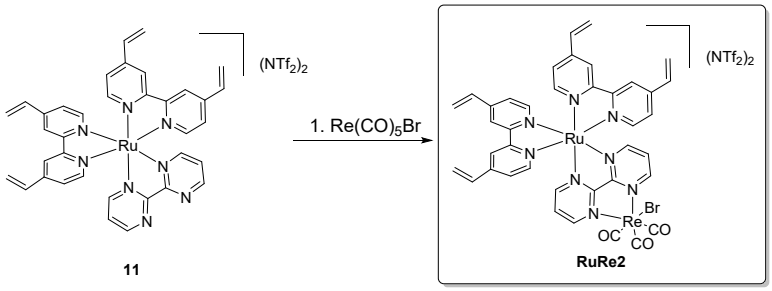

***Figure S16**: Synthesis of the RuRe2.*

RuRe 2: The synthesis was performed according to an adapted reported procedure.[7] 100 mg (0.08 mmol) of the Ru complex **11** and 65 mg (0.16 mmol) of $Re(CO)_5Br$ were refluxed in a 60 mL mixture acetone/ethanol 1:1 overnight. The solvent was evaporated and the solid was redissolved in the minimum amount of acetone and then precipitated with diethyl ether to obtain the pure **RuRe 2** in 59% isolated yield (74.2 mg). **^{1}H NMR** (400 MHz, Acetone-d_6) d: 5.76 (dt, J_{H-H} = 2.0, 10.8 Hz, 4H), 6.41 (m, 4H), 6.95 (m, 4H), 7.65 (m, 4H), 8.00 (m, 5H), 8.58 (d, J_{H-H} = 5.9 Hz, 1H), 8.79 (dd, J_{H-H} = 1.4, 5.6 Hz, 1H), 8.98 (m, 5H), 9.54 (dt, J_{H-H} = 1.5, 5.5 Hz, 2H). **^{13}C{^{1}H} NMR** (100.6 MHz, Acetone-d_6) d: 116.2, 119.4, 122.1, 122.3, 122.4, 122.6, 123.5, 123.6, 123.7, 125.1, 125.4, 125.6, 125.8, 127.1, 127.5, 134.0, 134.1, 134.2, 148.4, 148.5, 148.6, 152.9, 153.4, 154.2, 155.6, 158.0, 158.1, 158.4, 158.5, 160.0, 160.5, 162.4, 162.6, 162.7, 167.4, 167.8, 196.5. **ESI-HRMS:** Calculated for $C_{39}H_{30}BrN_8O_3ReRu^{2+}$. Exact: M^{2+}: 513.0107; Experimental: M^{2+}: 513.0099.

To confirm the coordination of the Re complex in the Ru complex **11** the same IR analysis performed for the **RuRe1** was performed for this complex. Was carried out an IR analysis of the complex before and after the coordination of the Re complex.

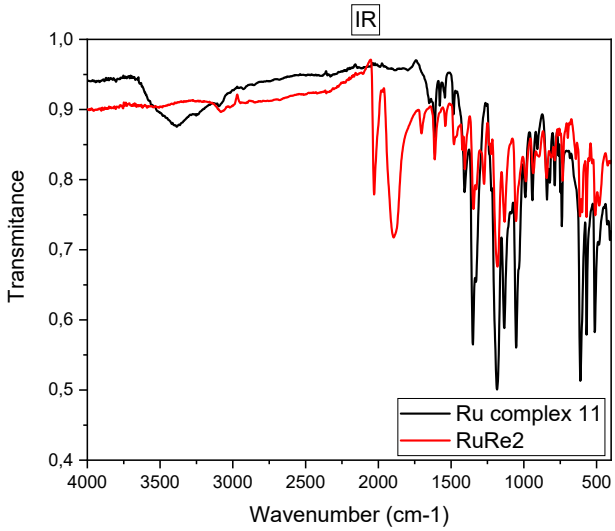

***Figure S17**: IR Spectrum of red) **RuRe2** black) Ru complex **11**.*

As observed for the **RuRe1** the same behavior is observed for the **RuRe2**. In the Figure S17 in the IR spectrum of the Ru complex **11** there are not any characteristic peak of the CO bond, instead when the Re complex is coordinated is possible to observe two peaks corresponding to the CO bond in 2030 and 1895 cm^{-1}. These peaks confirms that the Re complex is well coordinated to the Ru complex **11**.

SIX. Electropolymerization CV, FESEM images and EDX analysis:

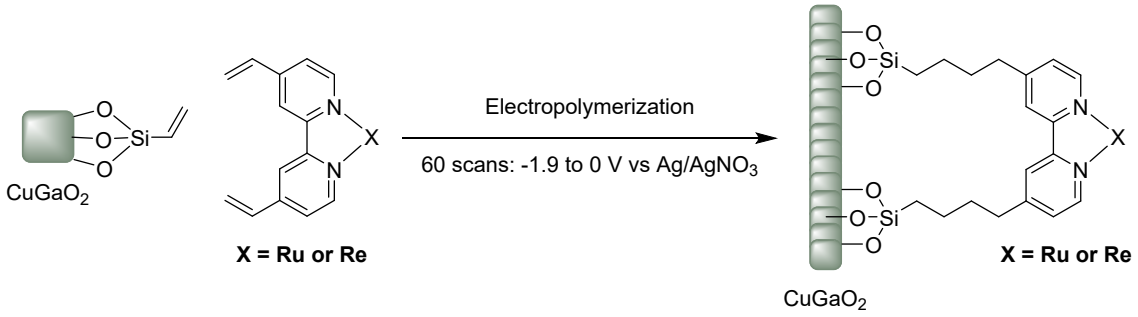

***Figure S18**: Electropolymerization of the molecular complexes scheme.*

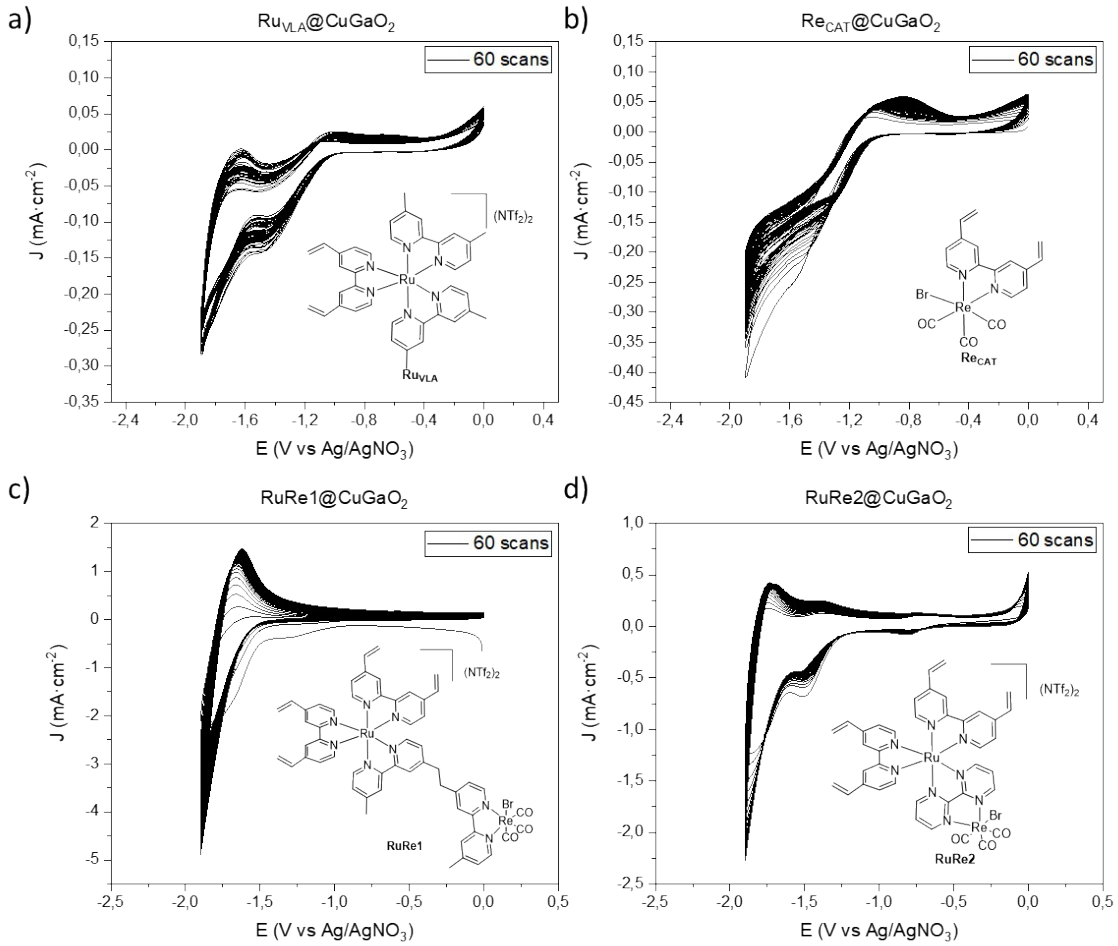

***Figure S19**: Cyclic voltammogram graphics of a) Electropolymerization of the **Ru_{VLA}** complex b) Electropolymerization of the **Re_{CAT}** complex. c) Electropolymerization of the **RuRe1** complex d) Electropolymerization of the **RuRe2** complex. All the CV are performed from 0 to -1.9 V vs Ag/$AgNO_3$ in an acetonitrile solution containing 0.1 M $Et_4N{\cdot}PF_6$ and 0.5 mM of the corresponding complex.*

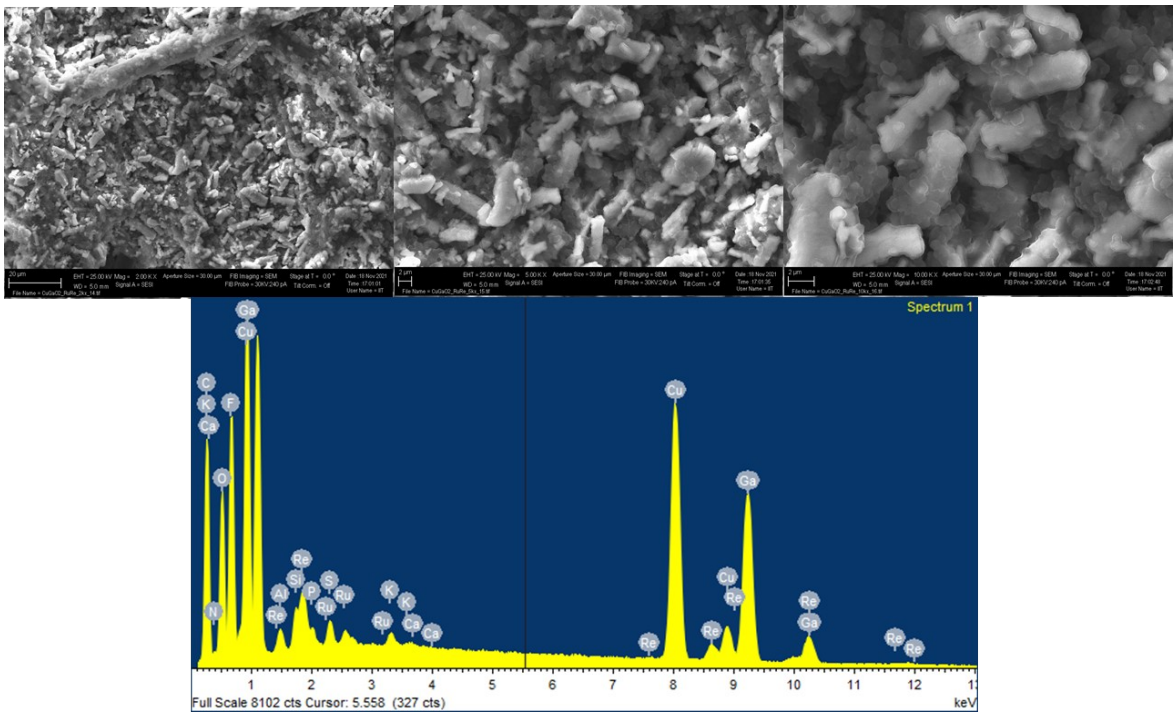

***Figure S20**: FESEM images and EDX analysis of the $CuGaO_2$ electrode after the electropolymerization of the **Ru_{VLA}** complex and **Re_{CAT}** complex (Ru+Re@$CuGaO_2$).*

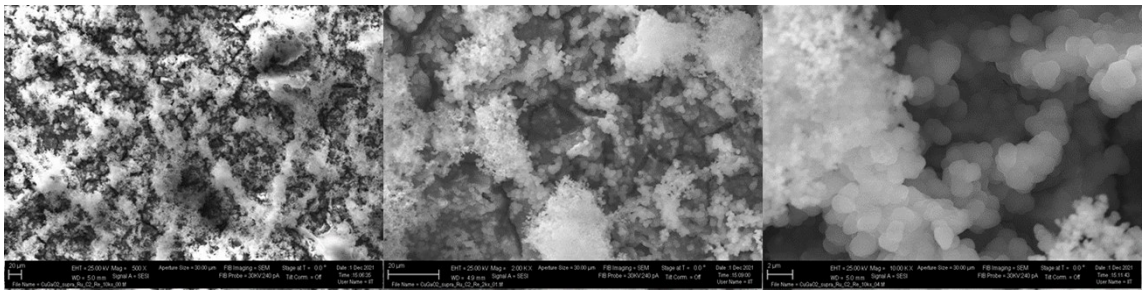

***Figure S21**: FESEM images of the $CuGaO_2$ electrode after the electropolymerization of the **RuRe1** complex (RuRe1@$CuGaO_2$).*

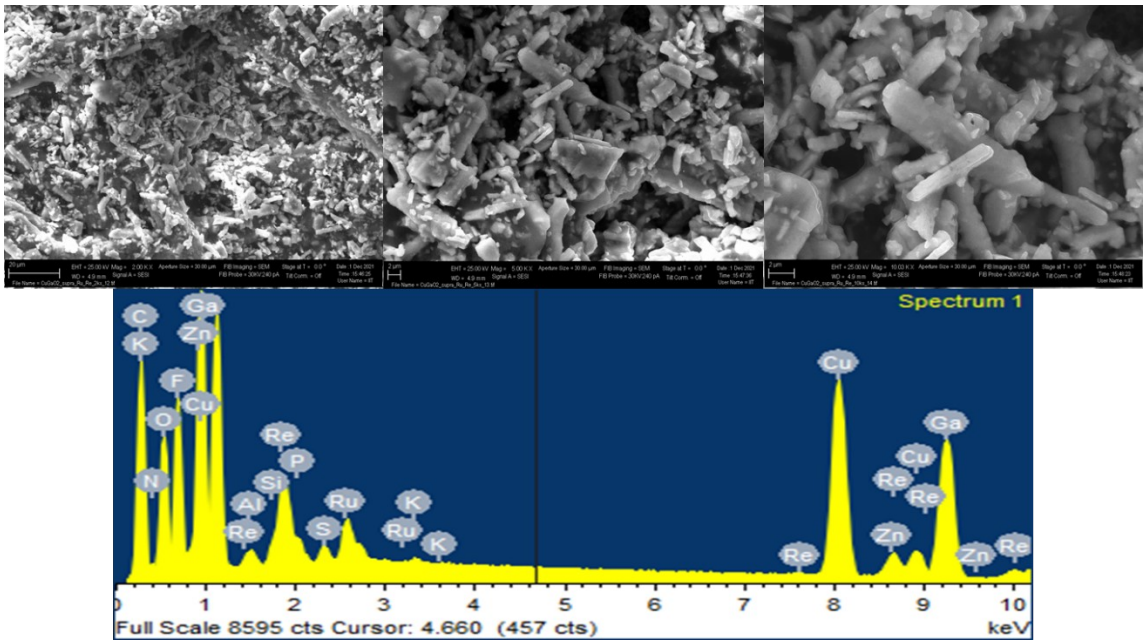

***Figure S22**: FESEM images and EDX analysis of the $CuGaO_2$ electrode after the electropolymerization of the **RuRe2** complex (RuRe2@$CuGaO_2$).*

SX. UV-Vis spectra of the molecular complexes

The UV-Vis of the different molecular complexes were performed to check the absorbance wavelength of each complex.

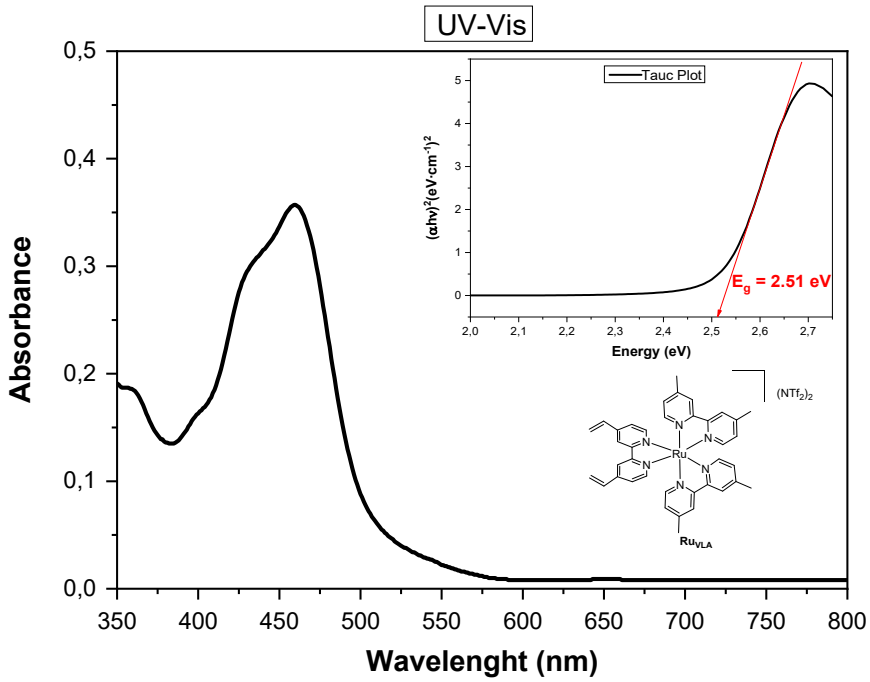

***Figure S23**: UV-Vis spectra and Tauc plot of the **Ru_{VLA}** complex.*

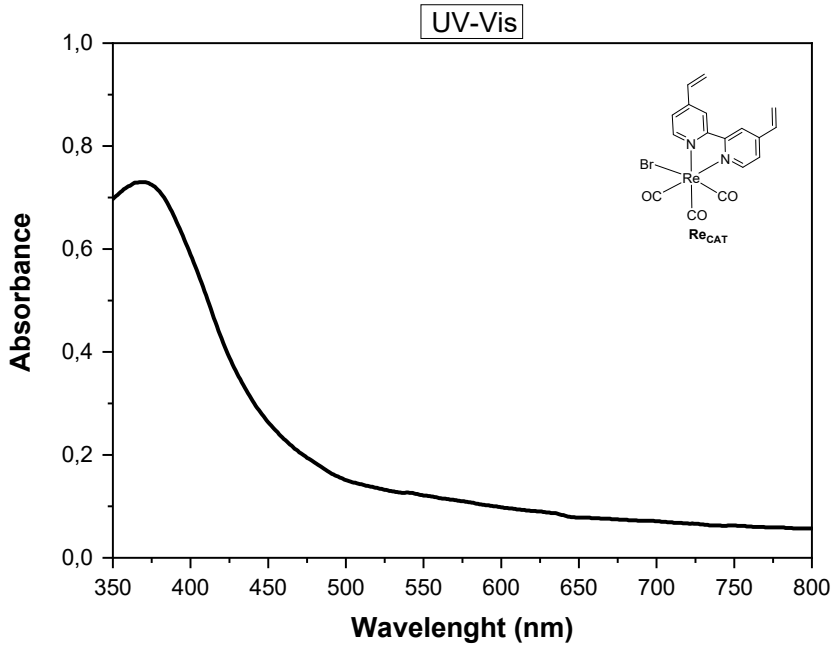

***Figure S24**: UV-Vis spectra and Tauc plot of the **Re$_{CAT}$** complex.*

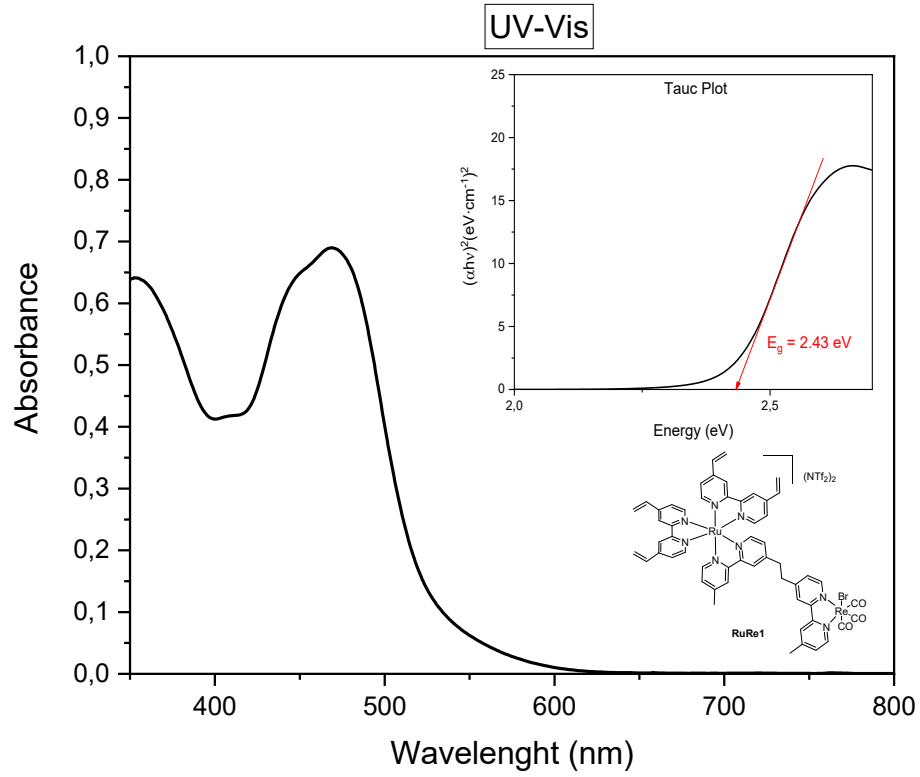

***Figure S25**: UV-Vis spectra and Tauc plot of the **RuRe1**.*

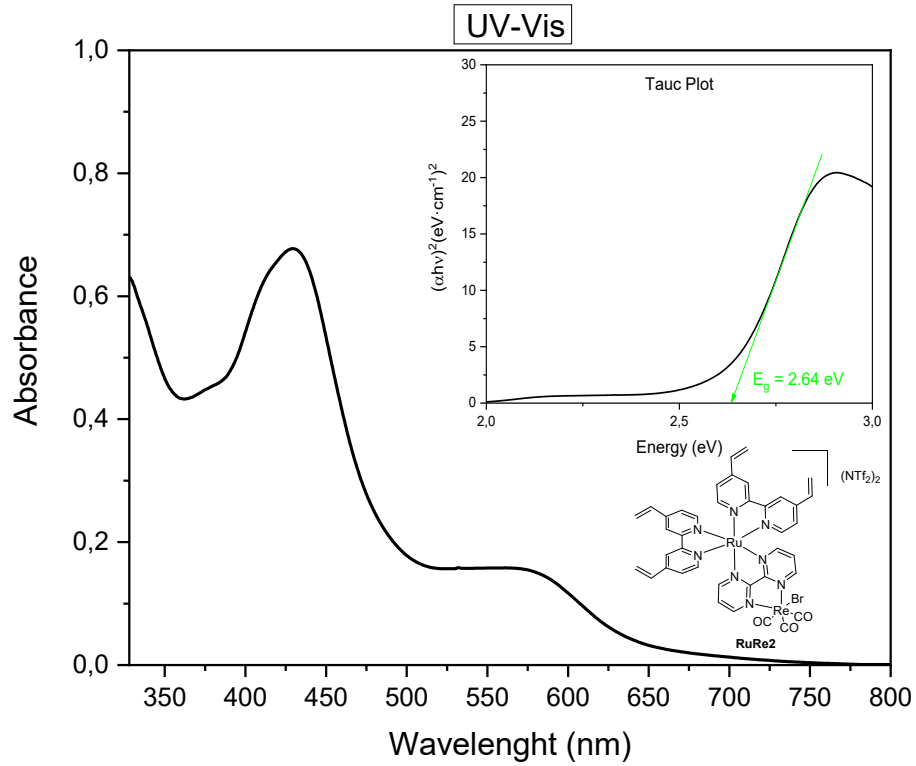

***Figure S26**: UV-Vis spectra and Tauc plot of the **RuRe2**.*

SXI. Cyclic voltammetry graphics

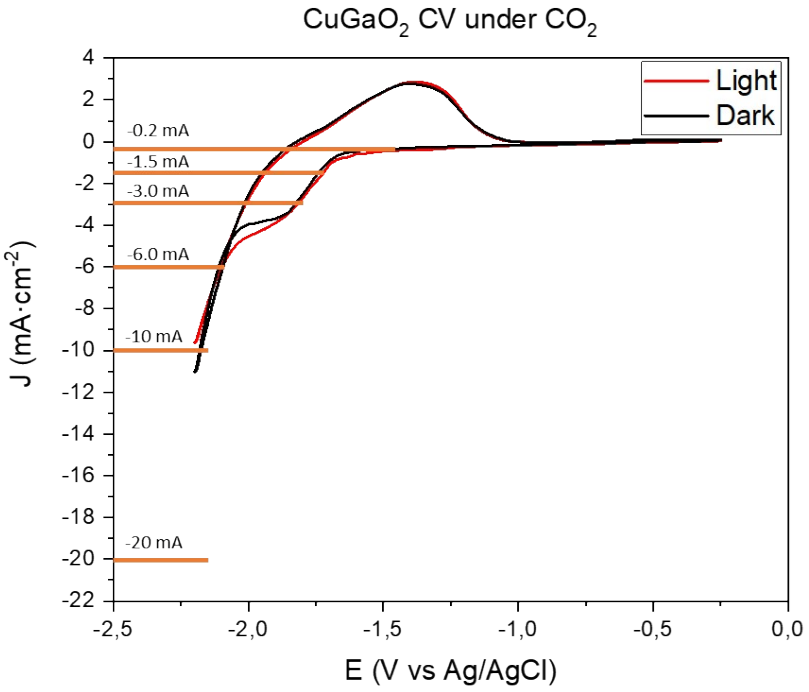

***Figure S27**: Cyclic voltammetry graphic of $CuGaO_2$ in an acetonitrile 0.3M BMIM·triflate solution CO_2 saturated with (red) and without (black) simulated sunlight irradiation.*

SXII. Results of all CO_2 reduction tests

***Table S1**: µmol of gas and liquid products produced in a 30 min chronopotentiometry at different current intensities in an acetonitrile 0.3 M BMIM·TfO solution saturated with CO_2 under simulated sunlight irradiation with different samples. Values in brackets are the Faradaic Efficiencies (%). [a]Experiments performed at dark conditions. [b]Experiment performed in an acetonitrile 0.3 M BMIM·TfO solution saturated with N_2.*

Sample	Current intensity (mA·cm^{-2})	µmol H_2	µmol CO	µmol Formate	µmol Methanol	µmol Ethanol	µmol 2-Propanol
[a]$CuGaO_2$	-0.2	0.81 (43)	-	-	-	-	-
[a]$CuGaO_2$	-1.5	1.24 (9)	3.49 (25)	5.64 (40)	0.05 (1)	0.12 (5)	0.11 (7)
[a]$CuGaO_2$	-3.0	1.14 (4)	6.08 (22)	9.51 (34)	-	0.11 (3)	0.13 (4)
[a]$CuGaO_2$	-6.0	1.58 (3)	9.92 (18)	10.67 (19)	0.06 (<1)	0.13 (1)	0.39 (6)
[a]$CuGaO_2$	-10.0	2.91 (3)	10.04 (11)	35.75 (38)	-	0.12 (1)	0.28 (3)
[a]$CuGaO_2$	-20.0	5.86 (3)	3.99 (2)	28.46 (15)	-	0.13 (<1)	0.29 (1)
$CuGaO_2$	-0.2	0.21 (11)	0.18 (10)	-	-	-	-
$CuGaO_2$	-1.5	3.29 (24)	1.97 (14)	5.57 (40)	-	-	0.02 (1)
$CuGaO_2$	-3.0	9.41 (34)	3.90 (14)	6.79 (24)	-	-	0.04 (1)
$CuGaO_2$	-6.0	18.31 (33)	10.09 (18)	24.17 (43)	-	-	0.09 (1)
$CuGaO_2$	-10.0	12.07 (13)	6.08 (7)	17.83 (19)	-	0.67 (4)	0.15 (1)
$CuGaO_2$	-20.0	14.95 (8)	24.11 (13)	18.88 (10)	-	0.56 (2)	0.24 (1)
[b]Ru+Re@$CuGaO_2$	-1.5	-	-	-	-	-	-
Ru+Re@$CuGaO_2$	-0.2	0.13 (7)	0.07 (4)	-	-	-	-
Ru+Re@$CuGaO_2$	-1.5	0.95 (7)	6.08 (43)	5.97 (43)	-	-	0.11 (7)
Ru+Re@$CuGaO_2$	-3.0	4.56 (16)	5.46 (20)	5.74 (21)	-	0.16 (3)	0.37 (12)
Ru+Re@$CuGaO_2$	-6.0	7.17 (13)	8.16 (15)	11.18 (20)	-	-	0.21 (3)
Ru+Re@$CuGaO_2$	-10.0	14.71 (16)	9.42 (10)	14.20 (15)	-	-	1.30 (13)
Ru+Re@$CuGaO_2$	-20.0	21.26 (11)	6.59 (4)	17.37 (9)	-	0.06 (<1)	1.42 (7)

***Table S2**: µmol of gas and liquid products produced in 120 min chronopotentiometry tests at -1.5 mA·cm^{-2}, under continuous simulated sunlight irradiation in an acetonitrile 0.3 M BMI·TfO CO_2 saturated solution using different samples. Values in brackets are the Faradaic Efficiencies (%). [a]Experiment performed at dark conditions. [b]Experiment performed in an acetonitrile 0.3 M $Et_4N·PF_6$ solution saturated with CO_2. [c]Experiment performed in an aqueous 0.1 M $KHCO_3$ solution saturated with CO_2.*

Sample	µmol H_2	µmol CO	µmol Formate	µmol Methanol	µmol Ethanol	µmol 2-Propanol
[a]$CuGaO_2$	5.81 (10)	4.95 (9)	20.55 (37)	0.07 (<1)	0.20 (2)	0.76 (12)
$CuGaO_2$	5.74 (10)	3.10 (6)	18.44 (33)	0.08 (<1)	0.04 (<1)	0.17 (3)
[b]Ru+Re@$CuGaO_2$	11.08 (20)	8.64 (16)	9.94 (18)	-	0.19 (2)	0.42 (7)
[c]Ru+Re@$CuGaO_2$	44.67 (80)	-	7.67 (14)	-	0.07 (1)	-
Ru+Re@$CuGaO_2$	7.70 (14)	3.25 (6)	24.49 (44)	0.06 (<1)	0.14 (2)	0.77 (13)
RuRe1@$CuGaO_2$	10.66 (19)	1.83 (3)	24.30 (43)	0.07 (<1)	0.22 (2)	0.33 (5)
RuRe2@$CuGaO_2$	8.98 (16)	3.25 (6)	19.50 (35)	-	0.09 (1)	1.45 (23)

SXIII. FESEM images and EDX analysis of the tested electrodes

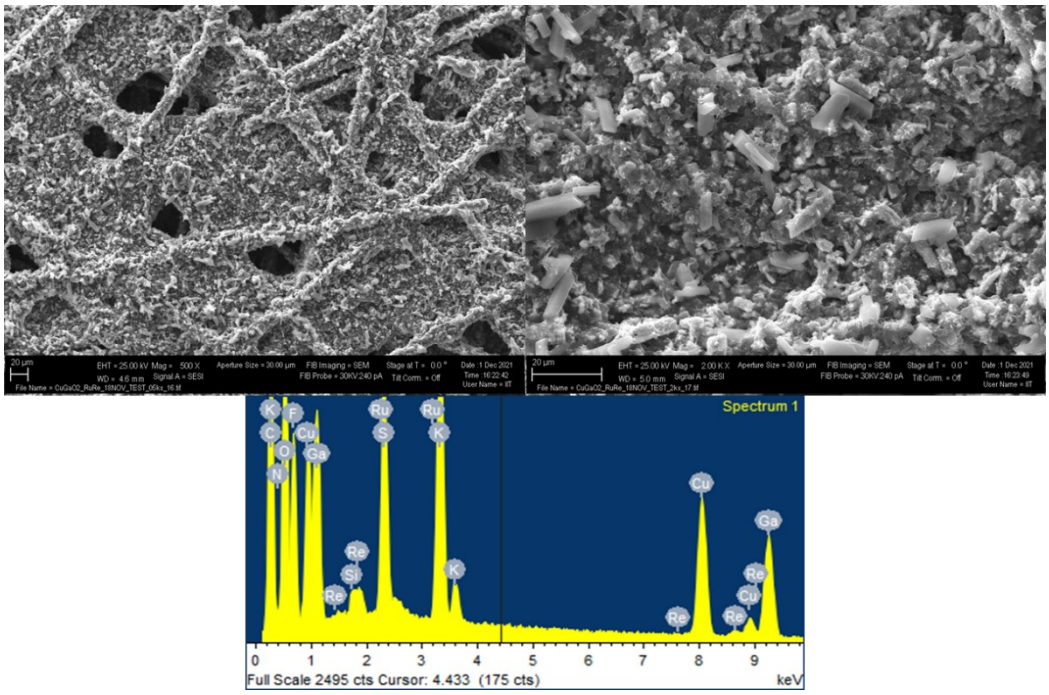

***Figure S28**: FESEM images and EDX analysis of the tested **Ru+Re@CuGaO$_2$** electrode.*

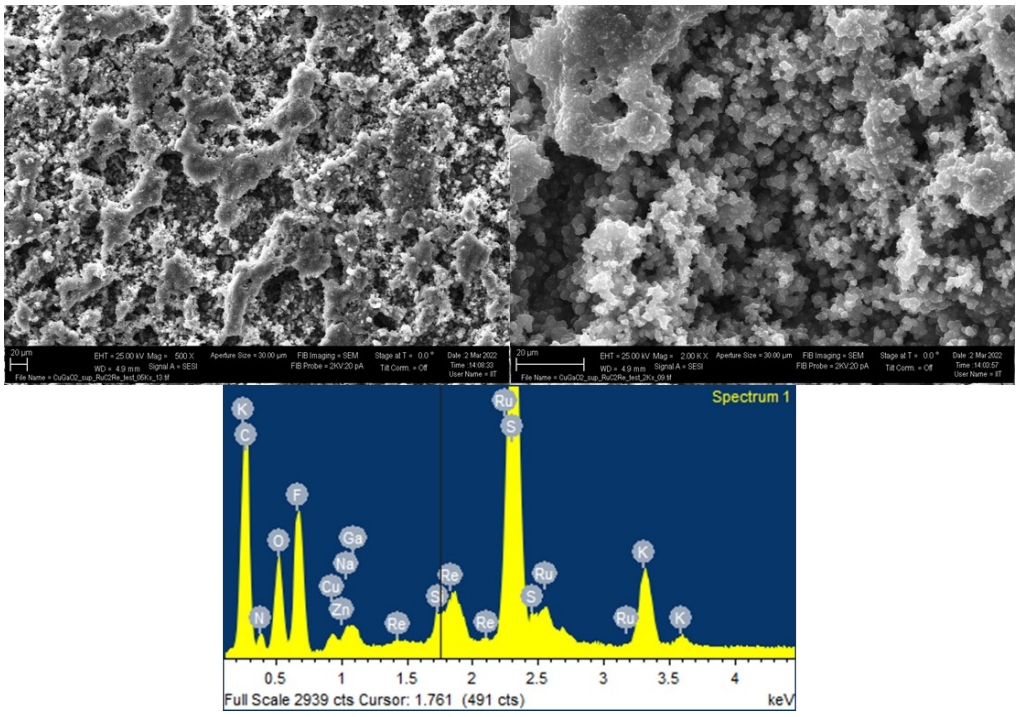

***Figure S29**: FESEM images and EDX analysis of the tested **RuRe1@CuGaO$_2$** electrode.*

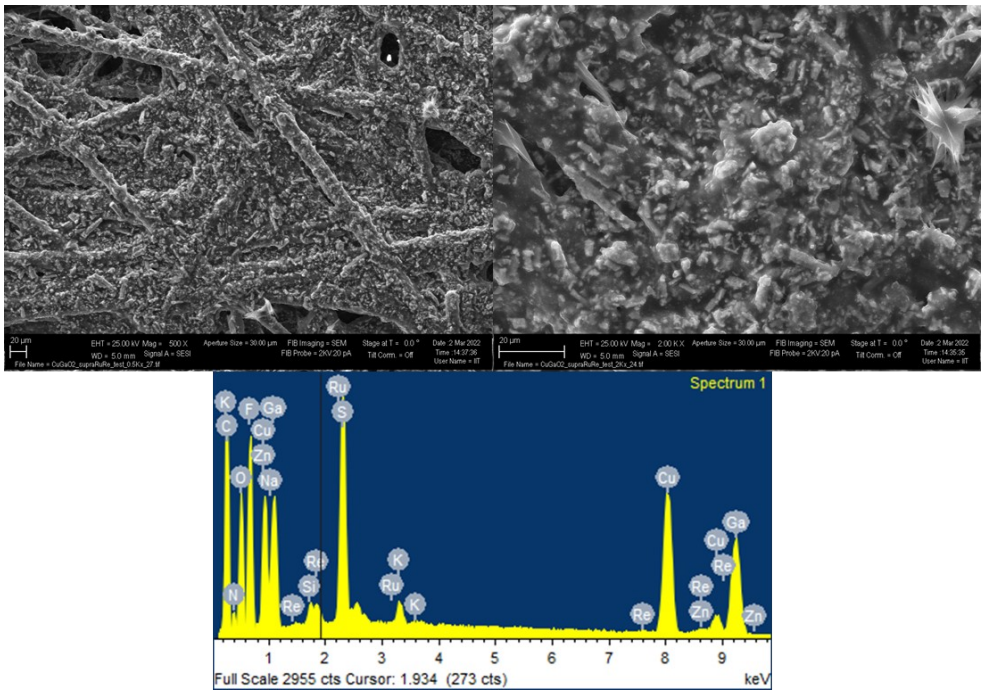

***Figure S30**: FESEM images and EDX analysis of the tested **RuRe2@CuGaO$_2$** electrode.*

SXIV. ^{1}H and ^{13}C NMR spectra

^{1}H NMR (CD_2Cl_2, 400 MHz)

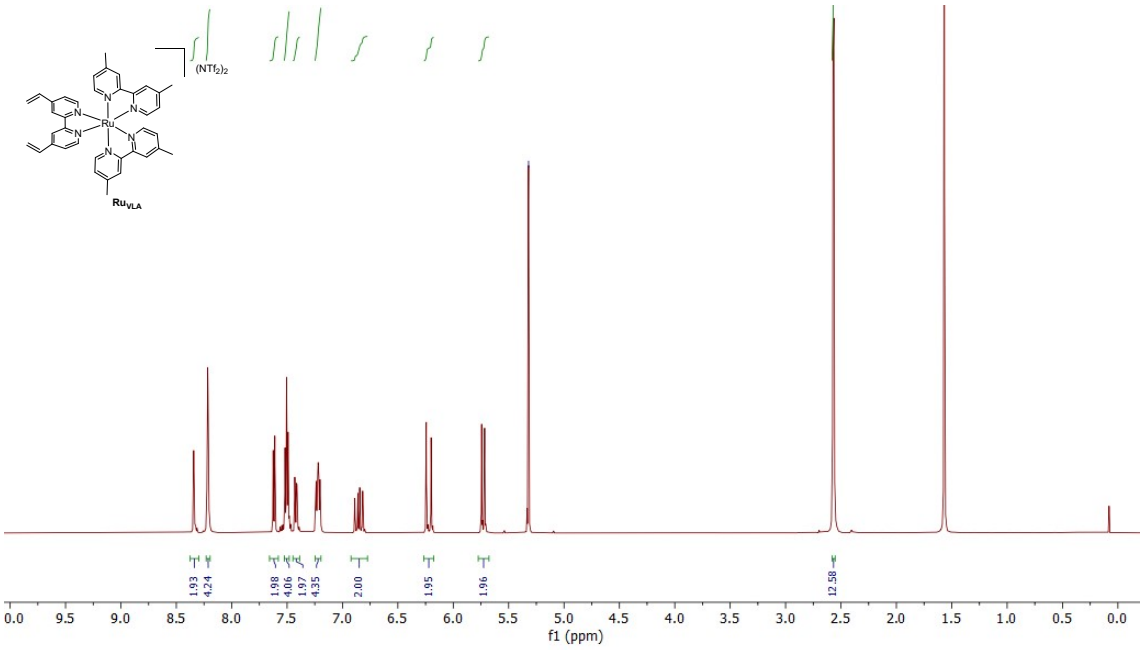

$^{13}C\{^{1}H\}$ NMR (CD_2Cl_2, 100.6 MHz)

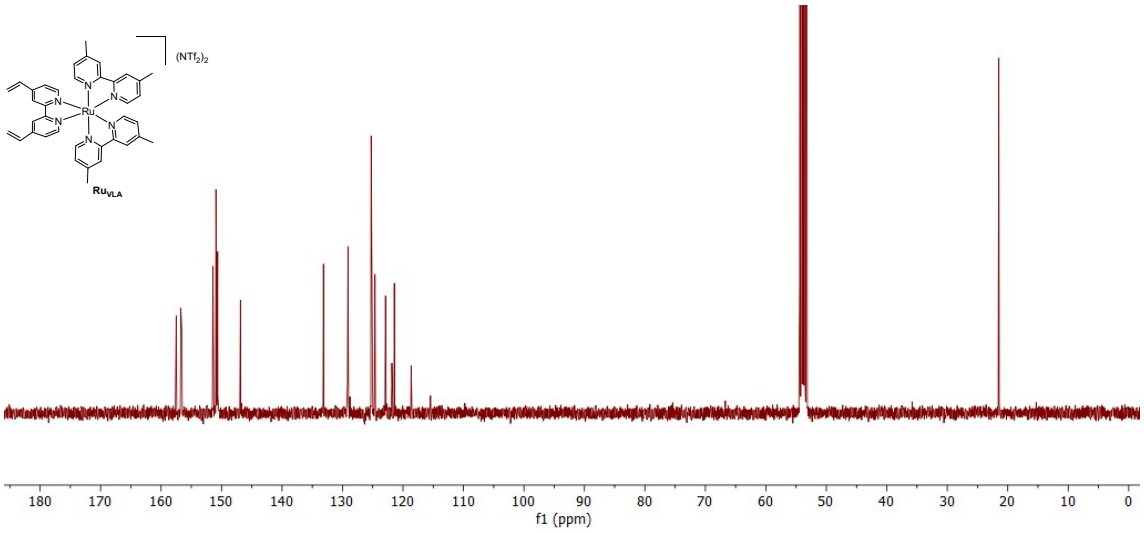

^{1}H NMR (dmso-d_6, 400 MHz)

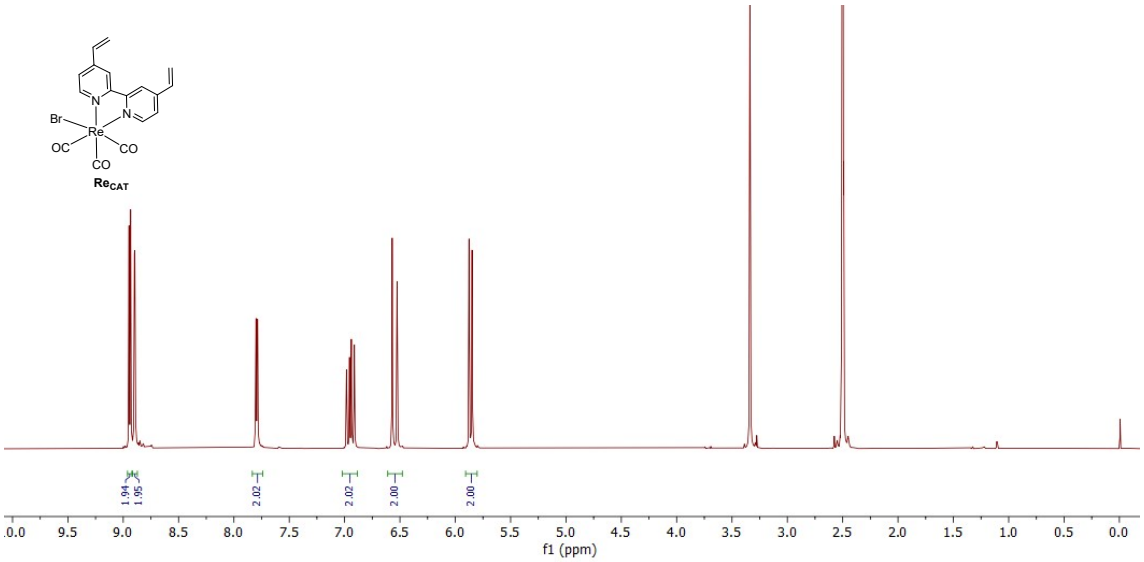

$^{13}C\{^{1}H\}$ NMR (dmso-d_6, 100.6 MHz)

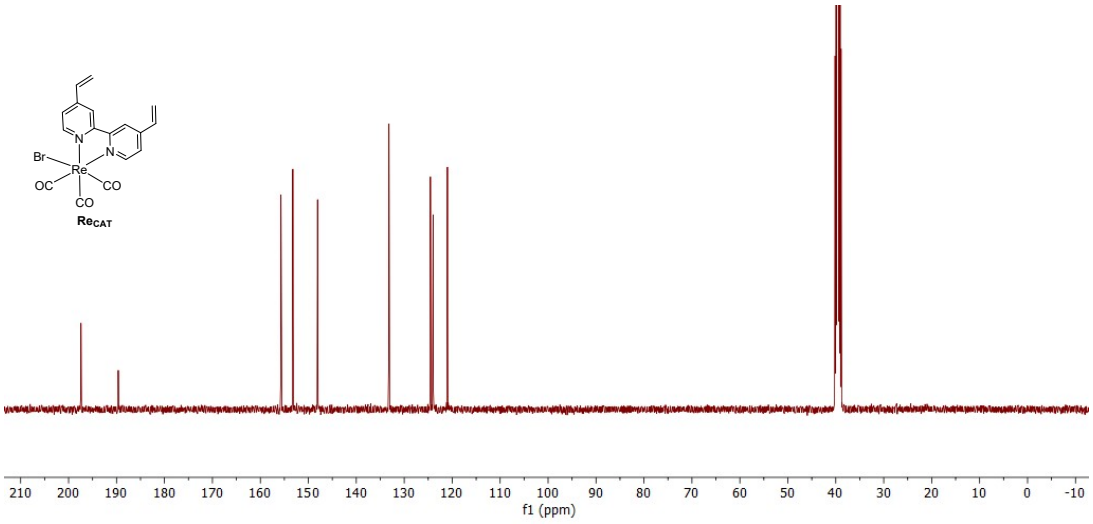

^{1}H NMR (CD_2Cl_2, 400 MHz)

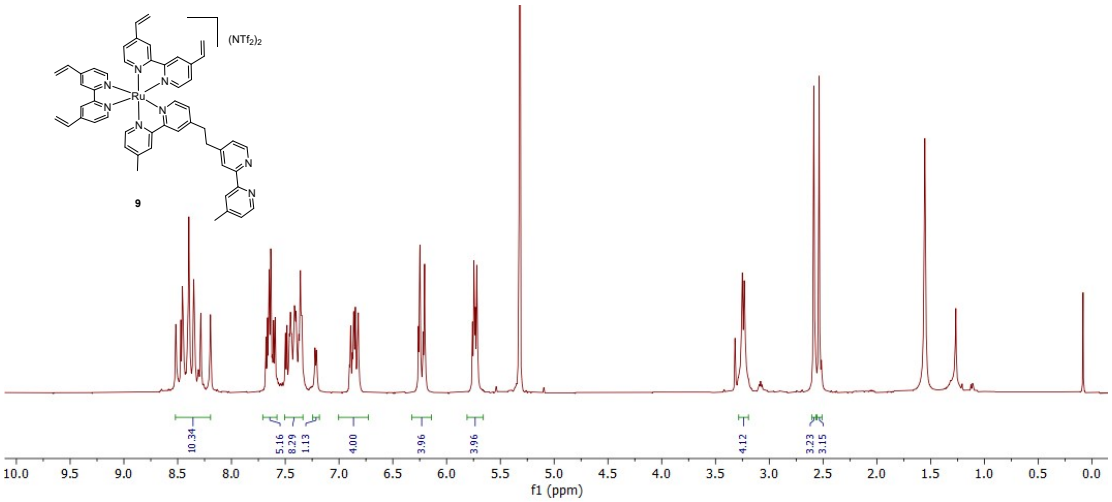

^{13}C{^{1}H} NMR (CD_2Cl_2, 100.6 MHz)

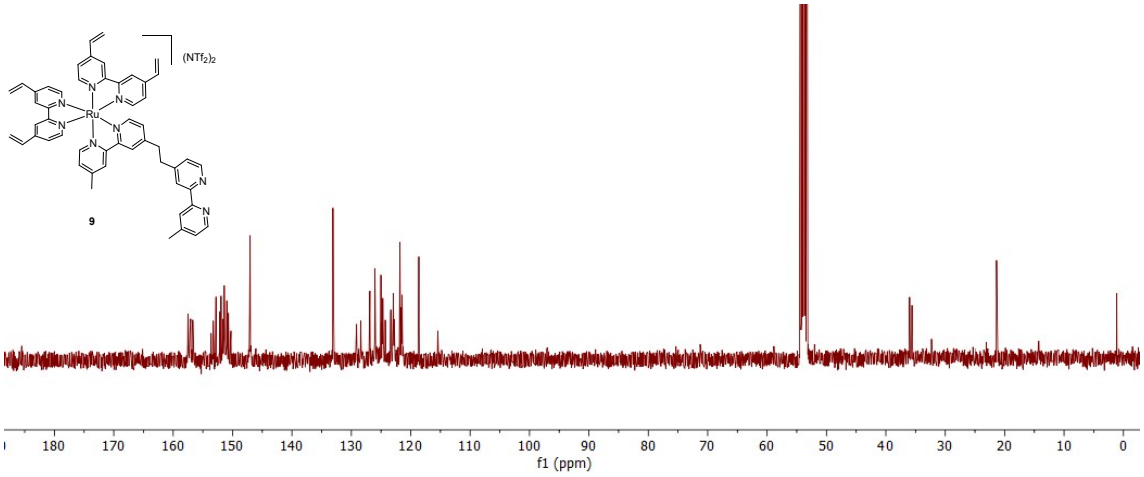

^{1}H NMR (CD_2Cl_2, 400 MHz)

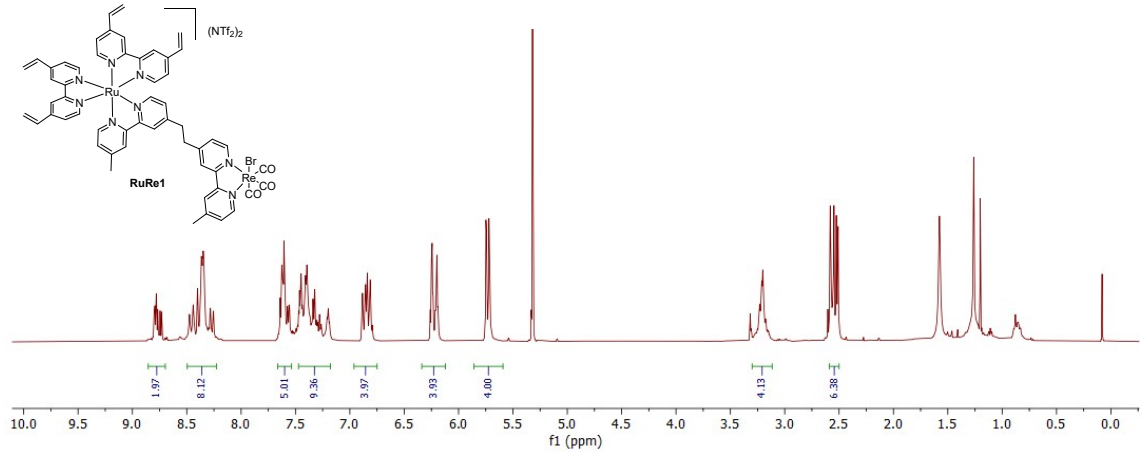

$^{13}C\{^{1}H\}$ NMR (CD_2Cl_2, 100.6 MHz)

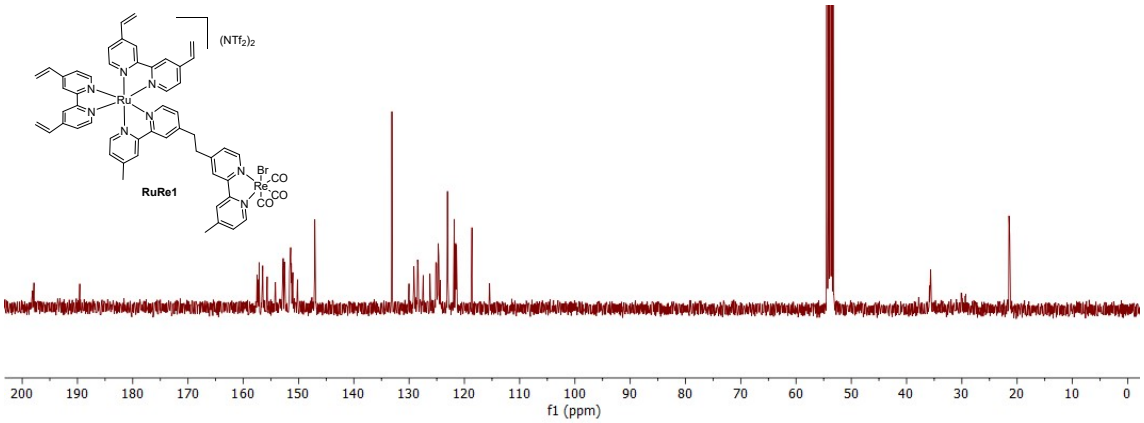

^{1}H NMR (CD_3OD, 400 MHz)

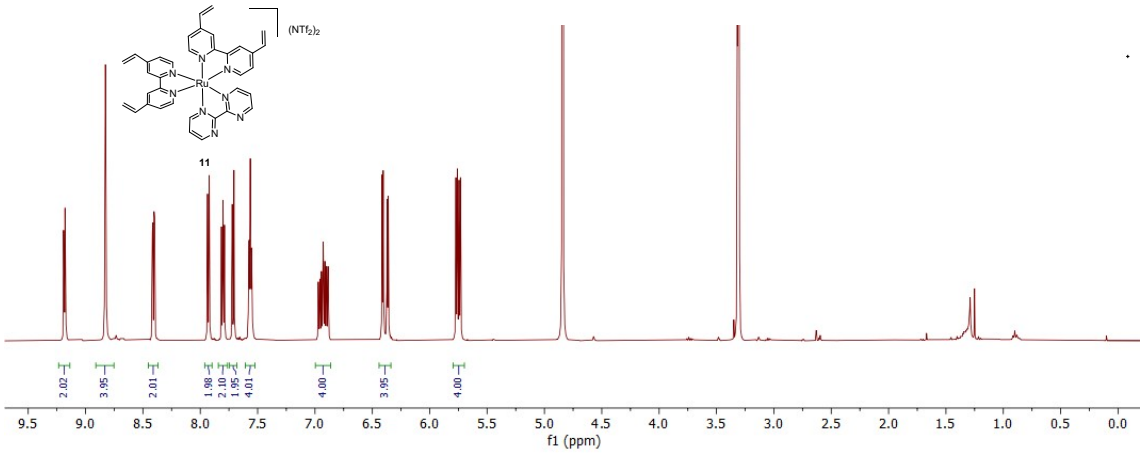

$^{13}C\{^{1}H\}$ NMR (CD_3OD, 100.6 MHz)

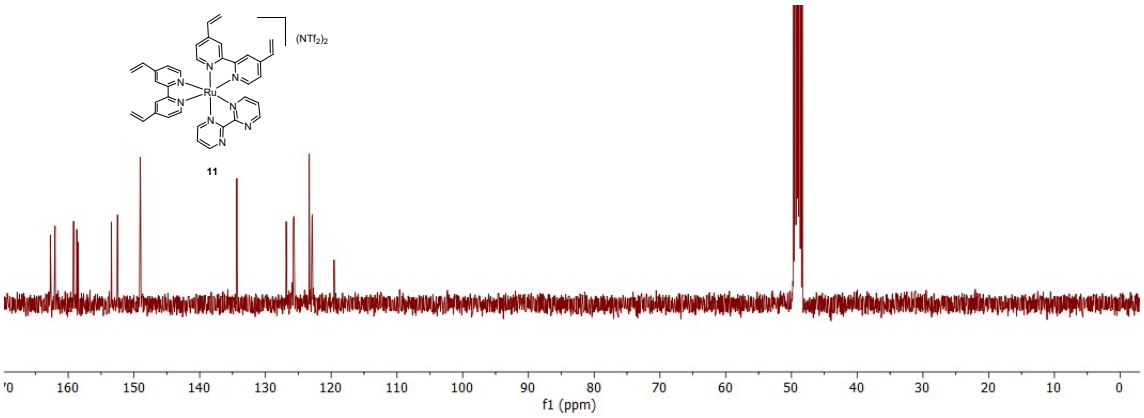

^{1}H NMR (acetone-d_6, 400 MHz)

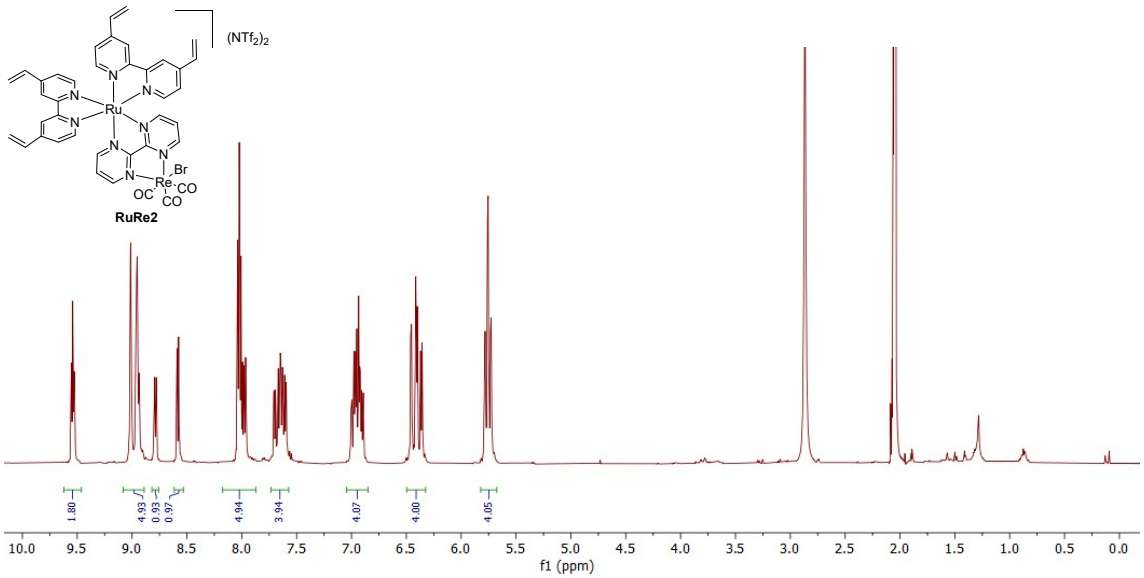

$^{13}C\{^{1}H\}$ NMR (acetone-d_6, 100.6 MHz)

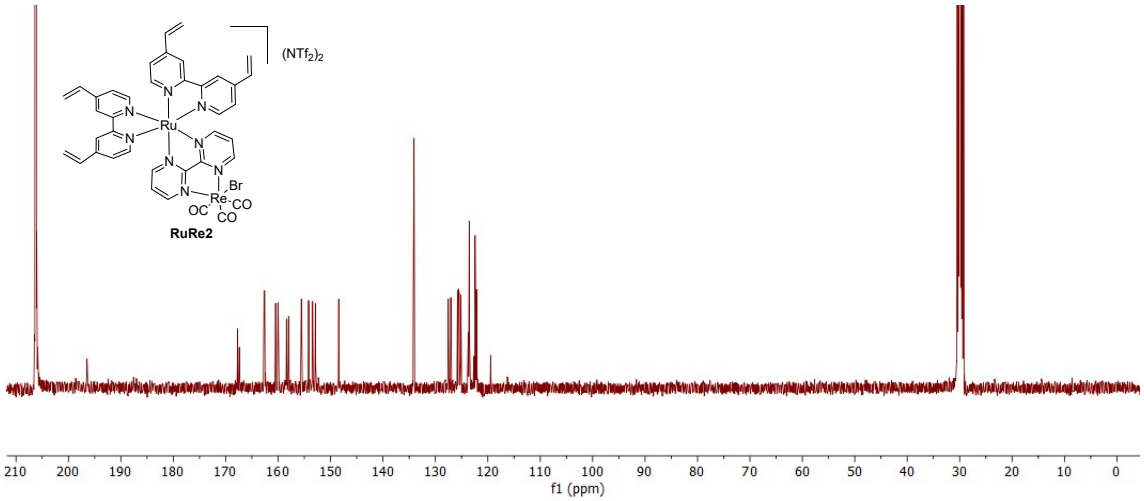

SXV. References

[1] J. Font, P. De March, F. Busqué, E. Casas, M. Benitez, L. Teruel, H. García, Periodic mesoporous silica having covalently attached tris(bipyridine) ruthenium complex: Synthesis, photovoltaic and electrochemiluminescent properties, J. Mater. Chem. 17 (2007) 2336–2343. https://doi.org/10.1039/b618773k.

[2] S. Meister, R.O. Reithmeier, A. Ogrodnik, B. Rieger, Bridging Efficiency within Multinuclear Homogeneous Catalysts in the Photocatalytic Reduction of Carbon Dioxide, ChemCatChem. 7 (2015) 3562–3569. https://doi.org/10.1002/cctc.201500674.

[3] M. Lee, D. Kim, Y.T. Yoon, Y. Il Kim, Photoelectrochemical Water Splitting on a Delafossite $CuGaO_2$, Bull. Korean Chem. Soc. 35 (2014) 3261. https://doi.org/10.5012/bkcs.2014.35.11.3261.

[4] A. Ito, Y. Matsui, Electrochemical and spectroscopic behaviors of a novel ruthenium(II) Complex with a Six-Membered Chelate Structure, Inorg. Chem. 58 (2019) 10436–10443. https://doi.org/10.1021/acs.inorgchem.9b00924.

[5] I. Gillaizeau-Gauthier, F. Odobel, M. Alebbi, R. Argazzi, E. Costa, C.A. Bignozzi, P. Qu, G.J. Meyer, Phosphonate-based bipyridine dyes for stable photovoltaic devices, Inorg. Chem. 40 (2001) 6073–6079. https://doi.org/10.1021/ic010192e.

[6] M. Braumüller, M. Schulz, M. Staniszewska, D. Sorsche, M. Wunderlin, J. Popp, J. Guthmuller, B. Dietzek, S. Rau, Synthesis and characterization of ruthenium and rhenium dyes with phosphonate anchoring groups, Dalt. Trans. 45 (2016) 9216–9228. https://doi.org/10.1039/c6dt01047d.

[7] A. Vogler, J. Kisslinger, Bipyrimidine-bridged rhenium(I)/rhenium(I) and ruthenium(II)/rhenium(I) complexes. Synthesis, electronic absorption and emission spectra, Inorganica Chim. Acta. 115 (1986) 193–196. https://doi.org/10.1016/S0020-1693(00)84413-8.